Measurement of thermal distortion in high power laser glass elements using ptychography

2015 Laser Phys. Lett. 12 025005

(http://iopscience.iop.org/1612-202X/12/2/025005)

IOP Publishing | Astro Ltd
Laser Physics Letters
Laser Phys. Lett. **12** (2015) 025005 (5pp)
doi:10.1088/1612-2011/12/2/025005

Measurement of thermal distortion in high power laser glass elements using ptychography

H Wang[1], Suhas P Veetil[2], C Liu[1], J Wang[1], W Huang[1], Y Zhang[1], X Pan[1] and J Zhu[1]

[1] Shanghai Institute of Optics and Fine Mechanics, Chinese Academy of Sciences, Shanghai 201800, People's Republic of China
[2] Department of Engineering Technology and Science, Higher Colleges of Technology, Fujairah 1626, UAE

E-mail: cheng.liu@hotmail.co.uk

Received 22 November 2014, revised 9 December 2014
Accepted for publication 11 December 2014
Published 9 January 2015

Abstract

The heat generated in the cavity of the high power slab laser amplifier makes it less stable and induces a thermal-lens effect which adds a spherical phase distribution to the wave-front of the laser beam. The commonly employed interferometry or Hartmann–Shack sensor based measurements are unable to provide an accurate measurement of the thermal distortion of the gain medium. It is demonstrated that this problem can be solved using a scheme based on ptychographical iterative engine. The complex transmittance of the outgoing laser is obtained by the proposed scheme while the amplifier is set at its turned off and turned on state and the thermal distortion caused by the pumping light is calculated from the obtained transmittance.

Keywords: phase retrieval, thermal distortion, ptychographical iterative engine, diffractive optics

(Some figures may appear in colour only in the online journal)

1. Introduction

In laser amplifiers working at high frequencies, the gain medium retains a certain amount of energy from pumping systems such as laser-diodes or flash lamps, which is essentially unwanted heat. The temperature gradient set up in the gain material as a result of heating can often give rise to undesirable outcomes such as thermo-optic or elasto-optic effects and bulk displacement [1]. They all adversely affect the beam quality by causing distortions to the laser wavefront. An accurate diagnostics of such wavefront distortions arising from thermal instabilities assumes much importance, as this information is of great use while trying to compensate such distortions later in the following optical setup in order to achieve high-quality laser output.

There are two established ways to get knowledge of thermal distortions; one employs a numerical model to calculate the thermal effect and the other uses a wavefront sensor to measure it directly. The most commonly adopted numerical method which is based on finite element analysis (FEA) simulates the working conditions of the amplifier slabs and calculates its thermal distortion [2]. However, for an accurate calculation we need to carefully consider factors such as the pumping uniformity, the geometric construction, the cooling gas characteristics, thermal characteristics of the laser medium, as well as the heat transfer coefficient. Any mistake in these parameters will lead to an error in the calculated result. However, an exact knowledge of all these factors is practically impossible and difficult to account for by numerical modeling alone. So a numerical method is only adopted in the initial stage to estimate the thermal effect while designing the amplifier. The Hartmann–Shack sensor is most commonly used for wavefront measurement in the field of high power lasers. However, for the high power laser amplifier the thermal

deformation of the gain medium will act like a thermal lens to add an additional spherical phase to the wavefront of the laser beam causing the focal spots of the micro-lens array to overlap with each other and become unresolvable. While interferometric methods have enough accuracy and resolution while working in a vibration isolated environment of constant temperature and moisture, such methods are practically not viable in this case as the cooling gas passes at a very high speed through different layers of the gain medium in the slab amplifier, thus causing vibrations and disturbance in the optical system [3]. When measuring the wavefront of the transmitted laser beam with an interferometer, the interference fringes will always vibrate drastically. Additionally, when the laser amplifier works at a high frequency, the thermal distortion of the gain medium will suffer a quite steep phase change at its edge and hence the interference fringe density will become too high to resolve for the interferometer [4]. These are the reasons why the interferometer cannot be used for the measurement of the thermal distortion of high a power laser amplifier. Measurement of the thermal distortion of the gain medium is always a big challenge in the field of high power lasers.

Coherent diffractive imaging (CDI), which retrieves the complex phase directly from the diffraction pattern intensity can be a better alternative for the phase measurement in the field of high intensity lasers. The CDI algorithm was first proposed by Gerchberg and Saxton [5] in 1971 and then developed by Fienup [6–8] and several variations of the CDI algorithm exist at present [9, 10]. In this letter, a well-known CDI method for short wavelengths, an extended ptychographical iterative engine (ePIE) [11] is applied to measure the wavefront distortion due to thermal gradient which is present in the gain medium. Ptychographical iterative engine (PIE) was first proposed by Rodenburg in 2004 to overcome the disadvantages of traditional CDI and has been extensively used in the field of visible light, electron and x-ray microscopy [12–17]. While the standard PIE algorithm requires a prior known illumination on the specimen to obtain its image, an ePIE algorithm proposed by Maiden in 2009 can bring out the accurate illumination function as well as specimen function simultaneously [11, 18]. The wavefront distortion resulting from the thermal gradient of the gain medium is obtained via the ePIE algorithm by measuring the wavefronts of the laser beam being transmitted from the amplifier at its turn-off and turn-on modes. A comparison of the two transmitted fields can tell us the thermal distortion occurred in the amplifier gain medium. Since PIE is not an interferometric method, the recorded diffraction intensity, which is used to reconstruct the transmitted field does not suffer from other environmental factors which usually affect any interference technique. At the same time, it can measure very steep phase changes. This way, the thermal distortions can be effectively measured with the ePIE algorithm, which is otherwise difficult with traditionally established methods.

2. Basic principle of ePIE

The principle of ePIE is outlined in figure 1. The object $O(r)$ under the illumination $P(r)$ is shifted accurately across the optical axis. A series of diffraction patterns I_n are recorded by the CCD kept behind the object while the object is scanned at various shifted positions. Reconstruction proceeds as follows:

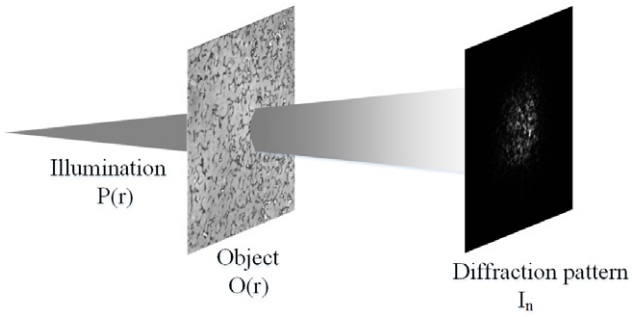

Figure 1. Principle of ePIE.

(a) The exit field at the current position R_i is calculated with two random guesses to $P_{n,g}(r)$ and $O_{n,g}(r, R_i)$

$$\Psi_{n,g}(r, R_i) = P_{n,g}(r) \cdot O_{n,g}(r, R_i) \tag{1}$$

where the subscript n, g represents a guessed function at the nth iteration.

(b) Corresponding wave function in the data recording plane is calculated from the Fourier transform of $\Psi_{n,g}(r, R_i)$

$$\Psi_{n,g}(k, R_i) = \mathfrak{F}\left[\Psi_{n,g}(r, R_i)\right] = \left|\Psi_{n,g}(k, R_i)\right| e^{i\theta_n(k, R_i)}. \tag{2}$$

(c) The amplitude of $\Psi_{n,g}(r, R_i)$ is replaced by the square root of I_n

$$\Psi_{n,c}(k, R_i) = \sqrt{I_n}\, e^{i\theta_n(k, R_i)} \tag{3}$$

where the subscript c represents the corrected wavefunction.

(d) The guess is updated at the exit field by inverse Fourier transform

$$\Psi_{n,c}(r, R_i) = \mathfrak{F}^{-1}\left[\Psi_{n,c}(k, R_i)\right]. \tag{4}$$

(e) The guessed illumination function and object function are updated with the following formulas

$$O_{n+1,g}(r, R_i) = O_{n,g}(r, R_i) + \frac{\left|P_{n,g}(r)\right|}{\left|P_{n,g}(r)\right|_{\max}} \frac{P_{n,g}{}^*(r)}{\left[\left|P_{n,g}(r)\right|^2 + \alpha\right]} \times \left[\Psi_{n,c}(r, R_i) - \Psi_{n,g}(r, R_i)\right] \tag{5}$$

$$P_{n+1,g}(r) = P_{n,g}(r) + \frac{\left|O_{n,g}(r, R_i)\right|}{\left|O_{n,g}(r, R_i)\right|_{\max}} \frac{O_{n,g}{}^*(r, R_i)}{\left[\left|O_{n,g}(r, R_i)\right|^2 + \alpha\right]} \times \left[\Psi_{n,c}(r, R_i) - \Psi_{n,g}(r, R_i)\right] \tag{6}$$

where $\left|P_{n,g}(r)\right|_{\max}$ and $P_{n,g}{}^*(r)$ are the maximum value of the amplitude and complex conjugate of $P_{n,g}(r)$ respectively, $\left|O_{n,g}(r, R_i)\right|_{\max}$ and $O_{n,g}{}^*(r, R_i)$ are the maximum value of the amplitude and complex conjugate of $O_{n,g}(r, R_i)$, and the value

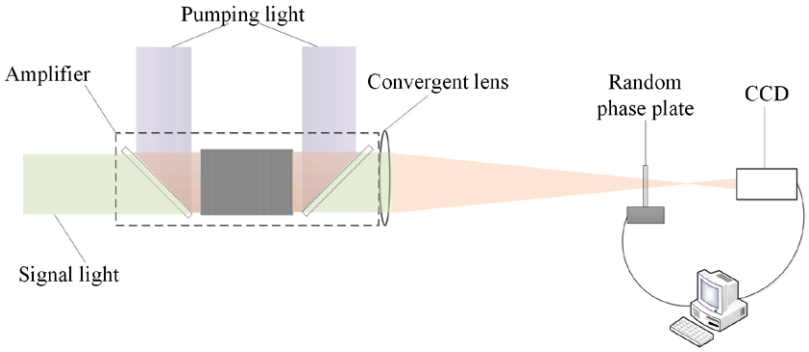

Figure 2. Experimental set up for the thermal distortion measurement of the amplifier.

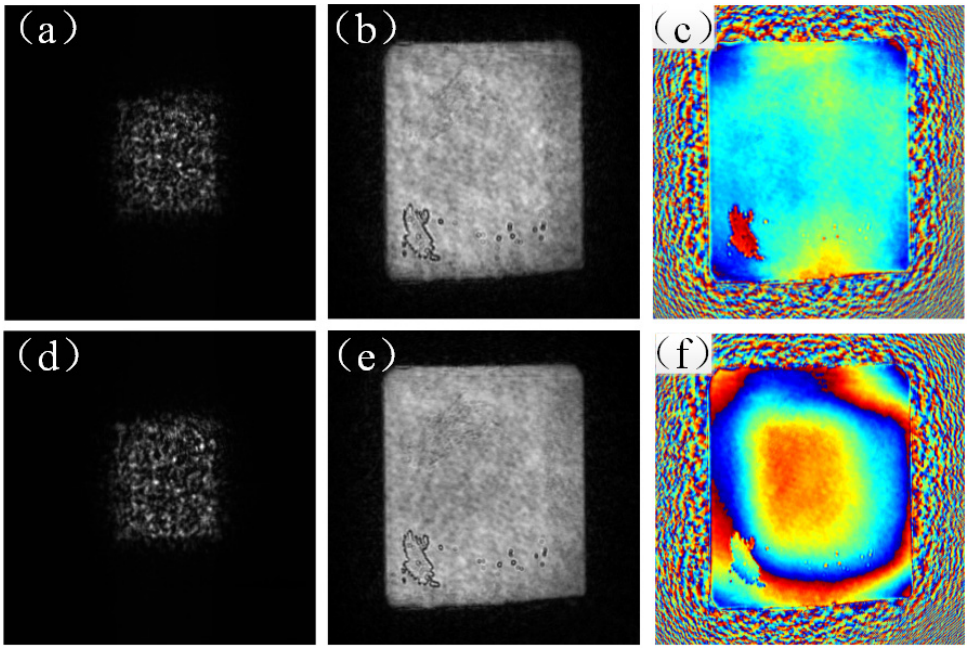

Figure 3. (*a*) One of the diffraction patterns recorded when the amplifier is turned off and the corresponding reconstructed modulus (*b*) and phase (*c*) at the amplifier exit; (*d*) one of the diffraction patterns recorded when the amplifier is turned on at 10 Hz and the corresponding reconstructed modulus (*e*) and phase (*f*) at the amplifier exit.

α is used to prevent a divide-by-zero occurring when $\left|P_{n,g}(r)\right| = 0$ or $\left|O_{n,g}(r, R_i)\right| = 0$.

Steps 1 to 5 are repeated until the differences in $O(r)$ and $P(r)$ in successive iterations are negligible.

3. Experiment

Figure 2 shows the schematic diagram of our prototype of a high frequency laser amplifier and the experimental setup for the measurement of the thermal distortion with the ePIE algorithm. The gain medium of the amplifier is composed of six Nd-glass slabs with size of 55 × 45 × 10.8 mm, space of 1 mm and the pumped area is 45 × 45 mm. The low energy laser with wavelength of 1053 nm is amplified under pumping with a laser diode with a wavelength of 802 nm and a pulse duration of 250 μs. The peak power of the laser diode is 48 kw and the pumping power on the amplifier is 150 W when the amplifier runs at 10 Hz and 600 W when the amplifier run at 40 Hz, 24% of which generate heat. To cool down the Nd-glass slabs, the helium gas flows through the gaps between these slabs at a high velocity to bring away most of the unwanted heat. However, the residual heat can lead to temperature differences between the center and the edge of the slabs and then non-uniform distortion will take place in the slabs and consequently twist the wavefront of the amplified laser beam.

The output from the amplifier is firstly focused by a convergent lens of 1000 mm in focal length and then made to fall on a random phase plate that can be stepped through the optics axis with the help of a step motor. This is shown in figure 2. During the raster scanning of the random phase plate $O(r)$ to a set of positions R_i the corresponding diffraction pattern formed on the CCD plane is recorded as I_n. Both the complex amplitude illuminating the scanning phase plate $P(r)$ and the complex transmittance of the phase plate $O(r)$ can be iteratively reconstructed from the diffraction pattern array I_n with the ePIE algorithm. By propagating the measured $P(r)$ numerically with the Fresnel formula to the front surface of the convergent lens, the complex amplitude of the beam $U(r)$ at the exit of the amplifier is obtained. If we assume

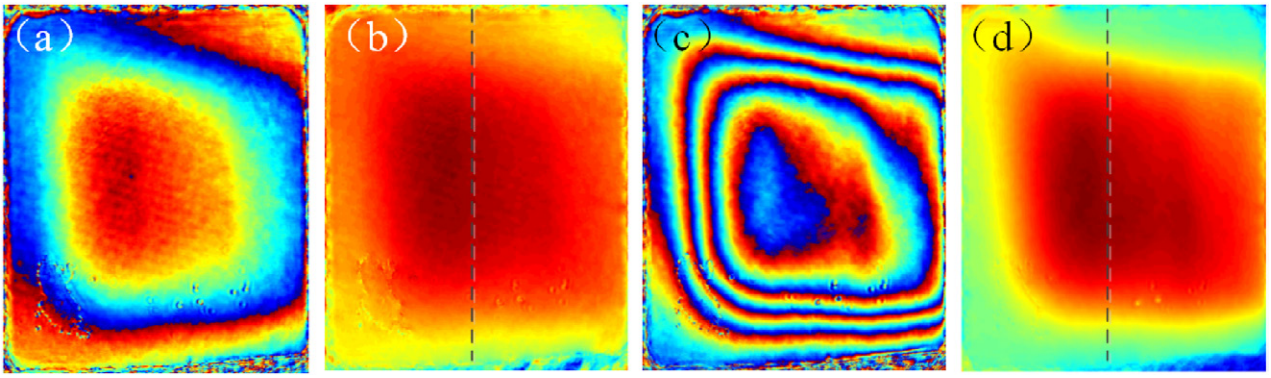

Figure 4. (*a*) wrapped phase distortion and (*b*) unwrapped phase distortion when the amplifier runs at 10 Hz, (*c*) wrapped phase distortion and (*d*) unwrapped phase distortion when the amplifier runs at 40 Hz.

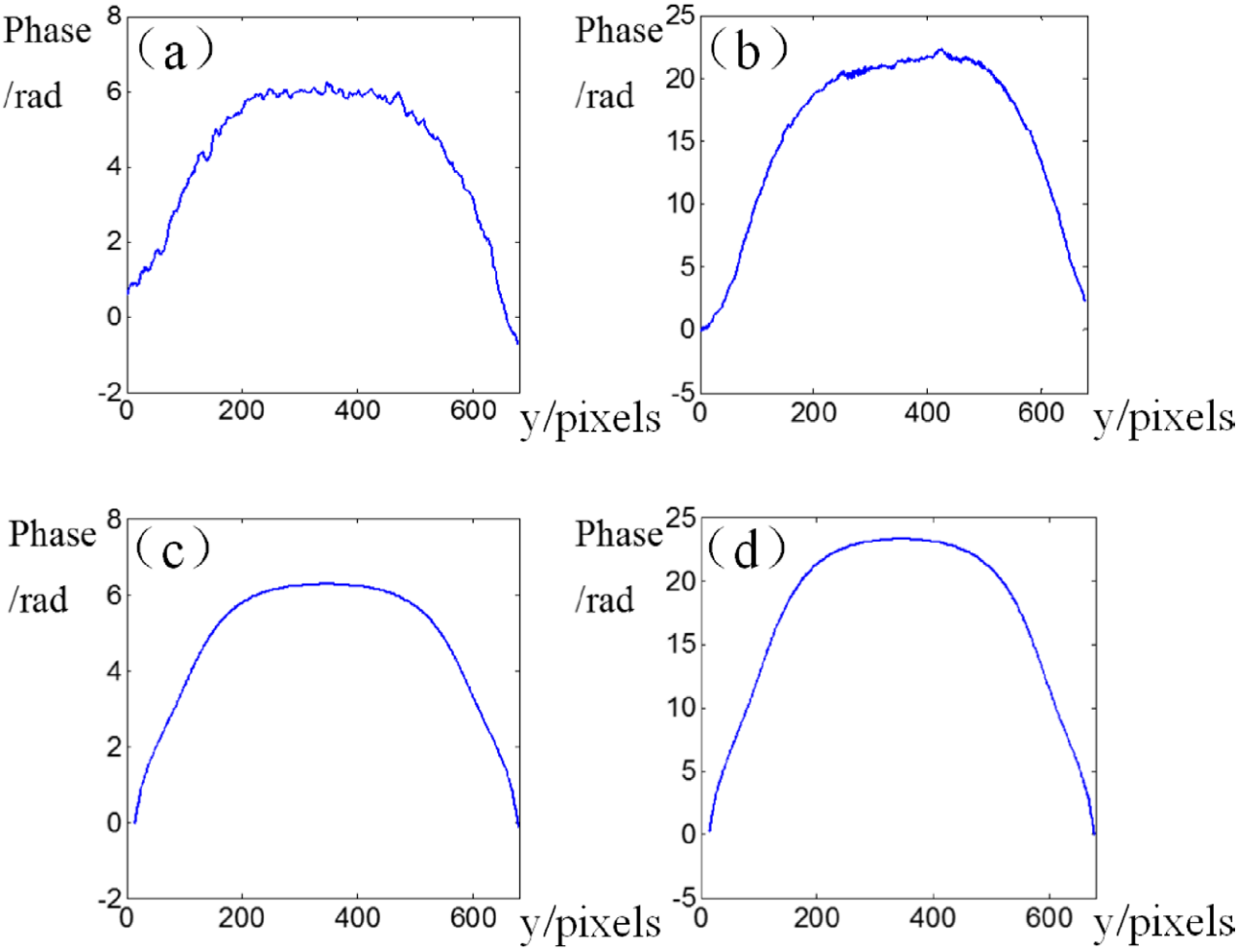

Figure 5. (*a*) Phase distortion within the pumped area taken along the vertical lines of figure 4(*b*), (*b*) phase distortion within the pumped area taken along the vertical lines of figure 4(*d*). (*c*) and (*d*) represent the corresponding thermal distortions calculated with FEA for the same area considered in (*a*) and (*b*).

the complex amplitude measured at the turn-off state as $U_0(r)$ and that measured at the running state as $U_1(r)$, the thermal distortion of the Nd-glass can be measured by calculating the phase difference between $U_1(r)$ and $U_0(r)$.

4. Results and discussion

Figure 3(*a*) is one of the 10 × 10 diffraction patterns recorded when the amplifier is turned off, figure 3(*b*) is the corresponding reconstructed modulus and figure 3(*c*) is the phase at the amplifier exit, where the tiny non-uniform phase background is because of the fact that the wavefront of the laser beam used is not ideally planar. Figure 3(*d*) is one of the 10 × 10 diffraction patterns recorded when the amplifier has run at 10 Hz for more than half an hour and the thermal deformation has become stable. Figures 3(*e*) and (*f*) are the corresponding reconstructed modulus and phase respectively. In comparison with figure 3(*c*), we can find that while the

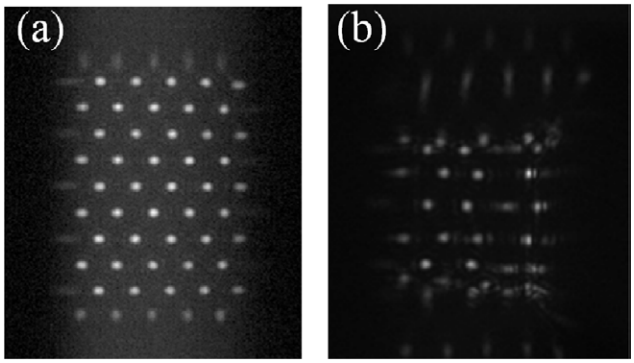

Figure 6. Focal spots of the micro-lens array recorded by the Hartmann–Shack sensor when the amplifier is (*a*) turned off and (*b*) turned on.

reconstructed modulus keeps almost the same distribution, there are obvious changes in phase, which has been caused by the thermal effect.

The phase change related to the thermal distortion is obtained by finding the phase difference between the phases obtained in figures 3(*f*) and (*c*) and is shown in figure 4(*a*). Figure 4(*b*) is the unwrapped phase of figure 4(*a*), where we can find that the Nd-glass slab becomes thicker at the central region due to the higher temperature at its center than the outside, forming the so called thermal-lens effect. Figures 4(*c*) and (*d*) are another set of experimental results when the amplifier works at 40 Hz. We can find that the thermal distortion with 40 Hz light pumping is much larger than that with 10 Hz light pumping.

For a distinct comparison, the values within the pumped area are taken along the vertical lines in figures 4(*b*) and (*d*) and are plotted in figures 5(*a*) and (*b*) respectively. The thermal distortions for a 10 Hz and 40 Hz pumping are calculated by the method of FEA in the same area as shown in figures 5(*a*) and (*b*) and are shown in figures 5(*c*) and (*d*). It is obvious that the wavefront deformation introduced by 10 Hz pumping light is about 6.1 rad(0.97 λ) while the wavefront distortion introduced by 40 Hz pumping light is about 22.1 rad(3.51 λ). This is understandable as the higher frequency pumping generates more heat inside the Nd-glass slabs than lower frequency pumping. Both results agree with the calculated values of thermal distortion, 6.2 rad(0.98 λ) with 10 Hz pumping light and 23.3 rad(3.71 λ) with 40 Hz pumping light, which are obtained by FEA method. The asymmetry in the measurement is caused by the non-uniformity of the pumping light, which is different from the condition taken for simulation. The spatial resolution of the measurement is calculated using $du = \lambda z / N\Delta p$, where z is the distance between the lens plane and the random phase plate, N is the number of pixels in the CCD used and Δp is the size of the each pixel. In the experiment the value of $N\Delta p$ is 1.5 cm, z is 945 mm and the wavelength is 1.053 μm. The spatial resolution determined by the above calculation is about 66 μm. It is obvious that this resolution is much higher than that of the Hartmann–Shack sensor, which is about several millimeters.

We have also measured the thermal distortion of the Nd-glass with the Hartmann–Shack sensor and the measurement results are shown in figure 6. Figure 6(*a*) shows the focal spots of the micro-lens array recorded by the Hartmann–Shack sensor in the turn-off state of the amplifier, while figure 6(*b*) shows the focal spots of the micro-lens array recorded as the amplifier is in the turned on state. It is shown in figure 6(*b*) that some of the focal spots have overlapped because of the thermal lens effect of the gain medium, and the results become unresolvable in this situation.

5. Conclusion

The ability of the proposed extended ptychographical itreative engine (ePIE) to measure steep phase changes while being immune to the thermal instabilities caused by the cooling system makes it an ideal technique for solving the problems in the measurement of thermal distortions of the Nd-glass in high frequency laser amplifiers. It provides a better option while we consider the limitations of most of the traditional wave-front sensor equipments. The feasibility of ePIE for this measurement is also demonstrated experimentally on our prototype of laser amplifier at frequencies of 10 Hz and 40 Hz and quite satisfying measurement results are obtained. To our knowledge, this is the first time that the ePIE algorithm is used in the field of high power laser amplifiers.

Acknowledgments

This research is supported by Grant GFZX0205010502.12 and Grant CXJJ-14-S104, China.

References

[1] Kuzmin A A, Khazanov E A and Shaykin A A 2011 *Opt. Express* **19** 14223
[2] Chow R, Ault L E, Taylor J R and Jedlovec D 1999 *Proc. SPIE* **3782** 246
[3] Sutton S B and Albrecht G F 1995 *Proc. SPIE* **2633** 272
[4] Wang H Y, Liu C, Veetil S P, Pan X C and Zhu J Q 2014 *Opt. Express* **22** 2159
[5] Gerchberg R W and Saxton W O 1972 *Optik* **35** 237
[6] Fienup J R 1978 *Opt. Lett.* **3** 27
[7] Fienup J 1979 *Opt. Eng.* **18** 529
[8] Fienup J 1980 *Opt. Eng.* **19** 297
[9] Zhang F, Pedrini G and Osten W 2007 *Phys. Rev.* A **75** 043805
[10] Zhang F and Rodenburg J M 2010 *Phys. Rev.* B **82** 121104
[11] Maiden A M and Rodenburg J M 2009 *Ultramicroscopy* **109** 1256
[12] Rodenburg J M and Faulkner H M 2004 *Appl. Phys. Lett.* **85** 4795
[13] Faulkner H M L and Rodenburg J M 2005 *Ultramicroscopy* **103** 153
[14] Hüe F, Rodenburg J M, Maiden A M, Sweeney F and Midgley P A 2010 *Phys. Rev.* B **82** 121415
[15] Humphry M J, Kraus B, Hurst A C, Maiden A M and Rodenburg J M 2012 *Nat. Commun.* **3** 730
[16] Weierstall U, Chen Q, Spence J C H, Howells M R, Isaacson M and Panepucci R R 2002 *Ultramicroscopy* **90** 171
[17] Chapman H N 2009 *Nat. Mater.* **8** 299
[18] Zhang F Peterson I, Vila-Comamala J, Diaz A, Berenguer F, Bean R, Chen B, Menzel A, Robinson I K and Rodenburg J M 2013 *Opt. Express* **21** 13592